2-Heteroaryl-[1,2,4]triazolo[1,5-c]quinazoline-5(6H)-thiones and their S-substituted derivatives: synthesis, spectral data and biological activity

Article *in* ChemPlusChem · January 2015

DOI: 10.1002/cplu.201500051R1

ChemPubSoc Europe

DOI: 10.1002/cplu.201500051

CHEMPLUSCHEM
Full Papers

2-Heteroaryl-[1,2,4]triazolo[1,5-*c*]quinazoline-5(6 H)-thiones and Their S-Substituted Derivatives: Synthesis, Spectroscopic Data, and Biological Activity

Andrii K. Bilyi,[a] Lyudmyla M. Antypenko,[a] Vitalii V. Ivchuk,[c] Oleksandr M. Kamyshnyi,[b] Natalya M. Polishchuk,[b] and Sergiy I. Kovalenko*[a]

In the continuing search for novel, biologically effective heterocyclic agents, several methods for the synthesis of 2-heteroaryl-[1,2,4]triazolo[1,5-*c*]quinazoline-5(6*H*)-thiones have been developed: thiolation of oxo derivatives, [5+1] cyclocondensation of [2-(3-heteroaryl-[1,2,4]triazol-5-yl)phenyl]amines with carbon disulfide, potassium ethyl xanthogenate, or aryl isothiocyanates, and in situ reaction of 2-isothiocyanatobenzonitrile with hydrazides. A series of *N*-*R*-2-[(2-heteroaryl-[1,2,4]triazole-[1,5-*c*]quinazoline-5-yl)thio]acetamides were obtained by aminolysis of the corresponding acetic acids and alkylation of potassium thiolates with *N*-*R*-2-chloroacetamides. It was established that some potassium thiolates, **4a**–**4d**, **4h**, and **4i**, had high antibacterial activity against *Staphylococcus aureus* with a minimum inhibitory concentration of 12.5 μg mL^{-1} and minimum bactericidal concentration of 25 μg mL^{-1}, which exceeded the values for trimethoprim. In addition, {2-[3-(1*H*-indole-2-yl)-1*H*-1,2,4-triazol-5-yl]phenyl}amine **2i** was investigated in the concentration range 100–0.01 μM at 59 lines of nine cancer cell types, and showed a mean effective concentration at 3.12–7.03 μM and cytotoxic effect at 15.56–67.38 μM. The possible mechanisms of activity were predicted by molecular docking studies to *S. aureus* dihydrofolate reductase and epidermal growth factor receptor kinase.

Introduction

Synthesis of novel biologically active compounds and their modification into highly efficient and low-toxicity drugs has always been one of the most important problems of modern pharmaceutical society. Particular interest is paid to heterocyclic compounds that combine in their structure the triazole and quinazoline heterocyclic systems, with pharmacological potential in the context of a "hybrid pharmacophore" approach.[1–6] Thus, quinazoline derivatives are used in medicine as effective anticancer (Afatinib, Lapatinib, Vandetanib, Anastrozole, and others), antifungal (Albaconazole), and antibacterial (Nifurquinazol) agents (Scheme 1).[7–9] There are also some antifungals (Itraconazole, Voriconazole, Terconazole, Fluconazole) and antiviral drugs (Ribavirin) among the triazole derivatives.[10–12]

The above data allow us to assume that condensing these two heterocycles and modifying their structure would enable us to find effective chemotherapeutic agents and to study their structure–activity relationship. Taking into account the results of our previous studies of sulfur-substituted [1,2,4]triazolo[1,5-*c*]quinazolin-2-yl-thione derivatives, which found the presence of antioxidant and antifungal (against *Candida albicans*) activities of the ([1,2,4]triazolo[1,5-*c*]quinazolin-2-ylthio)-carboxylic acids, as well as the expected positive impact of the heteroaryl pharmacophore on the target biological activity,[11] synthesis of the corresponding thiones and their structural modification at the fifth position could provide known pharmacological effects as well as causing the appearance of new, uninvestigated biological activities. Moreover, it is known that sulfur-containing compounds very often have antimicrobial activities, for example, some dithiocarbamic esters bearing a flavanone backbone, as well as their corresponding 1,3-dithiolium salts[13] or thiosulfinates, trisulfides, and benzylsulfinic acid from *Petiveria alliacea*,[14] had antibacterial properties against *Staphylococcus aureus* and *Escherichia coli*. Herein, the main methods for synthesis of the above heterocyclic systems are reviewed, and novel 2-heteroaryl-[1,2,4]triazolo[1,5-*c*]quinazoline-5(6*H*)-thiones were obtained for rapid biological activity prescreening and filtration of the data of large compound libraries for consequent structure optimization according their anticancer, antimicrobial, and antifungal activities.

[a] A. K. Bilyi, L. M. Antypenko, Prof. Dr. S. I. Kovalenko
Organic and Bioorganic Chemistry Department
Zaporizhzhya State Medical University
26 Mayakovsky Ave., 69035 Zaporizhzhya (Ukraine)
Fax: (+38) 0612-34-15-71
E-mail: kovalenkosergiy@gmail.com

[b] Dr. O. M. Kamyshnyi, N. M. Polishchuk
Microbiology, Virology, and Immunology Department
Zaporizhzhya State Medical University
31 Stalevariv Str., 69035 Zaporizhzhya (Ukraine)

[c] V. V. Ivchuk
Chemistry Department
Kryvyi Rih National University
11, the 22nd Partzyizd, 50027 Kryvyi Rih (Ukraine)

Supporting information for this article is available on the WWW under http://dx.doi.org/10.1002/cplu.201500051.

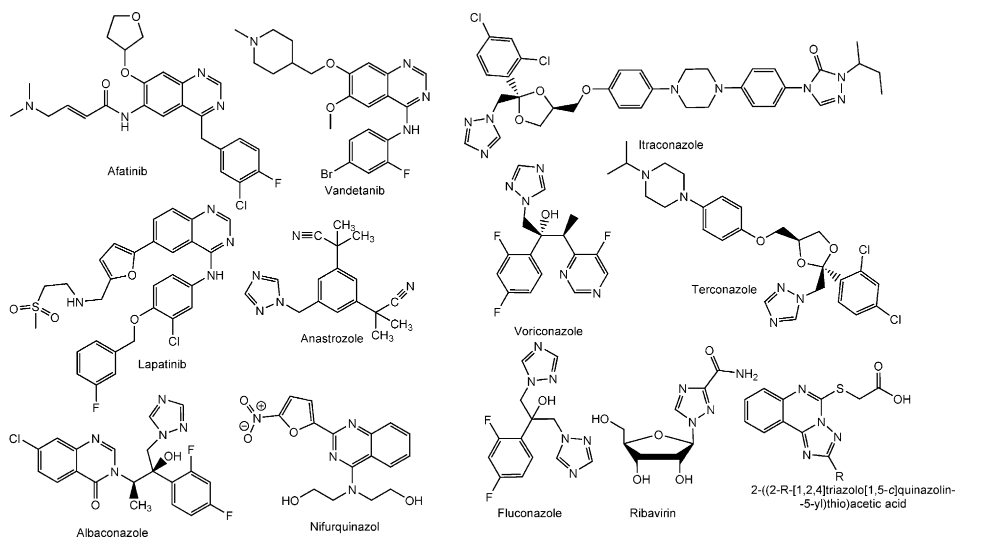

Scheme 1. Quinazoline and triazole derivatives with anticancer, antifungal, and antimicrobial activities.

Results and Discussion

Chemistry

Synthesis of 2-heteroaryl-[1,2,4]triazolo[1,5-*c*]quinazoline-5(6*H*)-thiones **3** was performed by treatment of oxo derivatives **1** with phosphorus pentasulfide in xylene (method A, Scheme 2). Owing to the moderate yields of final products **3** (54–76%), a number of alternative methods were used: interaction of amines **2** with carbon disulfide in the presence of potassium hydroxide in ethanol (method B), with potassium ethyl xanthogenate in 2-propanol (method C), and with phenyl isothiocyanate and acetic acid in 2-propanol (method D, Scheme 2).

The last method had several disadvantages and could not be used as a preparative technique. Thus, according to the LC–MS data, the reaction of amines **2** with phenyl isothiocyanate in 2-propanol formed a mixture of products: the original amine **2**, the corresponding thiourea, and thione **3** in ratio 2:7:1. The increase of the boiling point led to the corresponding thiones **3** with 58–62% yields according to the LC–MS data. The most successful preparative technique was method C with quantitative yielding of thiolates **4**, which were then readily transformed into the corresponding thiones **3** by the addition of hydrochloric acid solution (see the Supporting Information).

Additionally, an attempt at in situ formation of tandem thiones **3** by reaction of 2-isothiocyanatobenzene **5** with heteroarylcarboxylic acid hydrazides in dimethylformamide (DMF) (method E) was performed. In this case the individual thiones **3a**, **3d**, and **3g** were obtained with 55–62% yields (Scheme 3).

As a logical continuation of a systematic search for bioactive compounds with chemotherapeutic activity, and aiming to study the structure–activity correlation, a series of 2-(3-heteroaryl-[1,2,4]triazolo[1,5-*c*]quinazoline-5-ylthio)acetic acids **6** and their amides **7** were synthesized. Synthesis of acids **6** was performed by alkylation of the corresponding potassium thiolates **4** with chloroacetic acid in water or alcohol/water mixtures with an equimolecular amount of sodium hydroxide (method A, Scheme 4). After acidification of the reaction medium to pH 3–4, the corresponding acids **6** were isolated with 58–74% yields. The corresponding thiones **3** were also easily alkylated with chloroacetic acid in alcohol solution with addition of an equivalent amount of potassium hydroxide (method B, Scheme 4).

Alkylation of potassium thiolates **4** with *N*-cycloalkyl-(cyclyl, benzyl, aryl, heteroaryl)-2-chloroacetamides went smoothly without abnormalities in 2-propanol or dioxane. Note that alkylation lasted for 60–90 minutes in all cases, and the extension of its duration did not significantly affect the yield of amides **7** (method C, Scheme 4). Additionally, an alternative method of amide **7** synthesis was

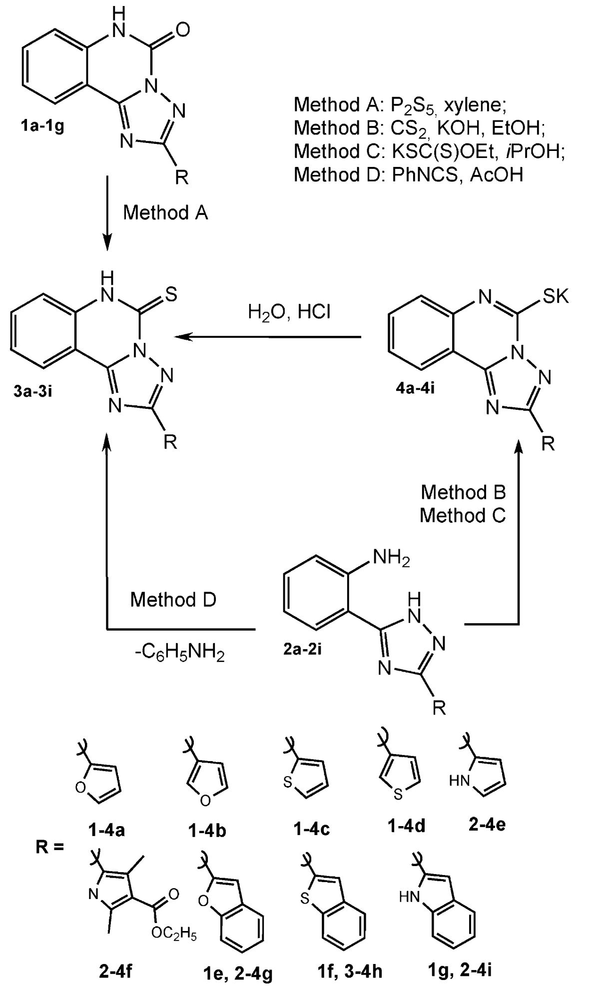

Scheme 2. Synthesis of 2-heteroaryl-[1,2,4]triazolo[1,5-*c*]quinazoline-5(6*H*)-thiones.

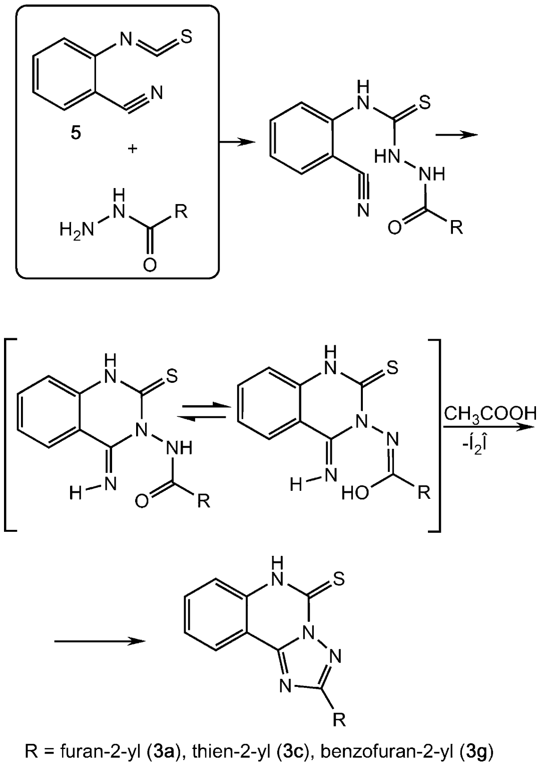

Scheme 3. Tandem formation of 2-heteroaryl-[1,2,4]triazolo[1,5-*c*]quinazoline-5(6*H*)-thiones.

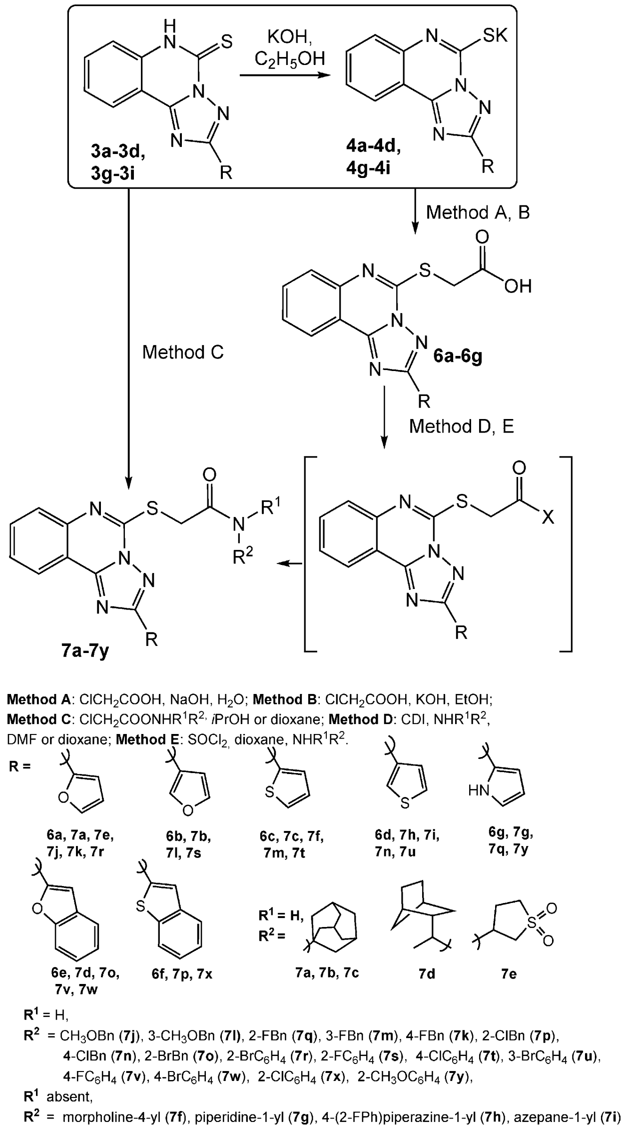

Scheme 4. Synthesis of 2-(3-heteroaryl-[1,2,4]triazolo[1,5-*c*]quinazoline-5-ylthio)acetic acids **6** and *N*-*R*-2-[(2-heteroaryl-[1,2,4]triazolo[1,5-*c*]quinazoline-5-yl)thio]acetamides **7**. Bn = benzyl.

performed, namely, aminolysis of the previously activated acids **6**. As activating components, *N,N'*-carbonyldiimidazole (CDI) or thionyl chloride were selected. The experiments showed that the corresponding imidazolides (method D) and chloroanhydrides **6** (method E) were formed quite easily and with high yields (Scheme 4). Importantly, their reactivity towards N-nucleophiles was sufficient for complete conversion into the corresponding amides **7** over 2–6 hours.

The individuality and structure of the compounds were confirmed by elemental analysis and physicochemical methods. In the LC–MS spectra of compounds the intense molecular ion peaks [*M*+1] and [*M*+2] were registered and confirmed the expected molecular weight of the synthesized compounds. The latter one characterized the "isotopic profile" of sulfur.

The IR spectra of compounds **3** had high-intensity stretching vibrations of the $\nu_{C=S}$ group of the thiolactamic bond at 1662–1627 cm^{-1}, and peaks of ν_{NH} at 3488–3175 and 3190–3111 cm^{-1}, which is the Raman band oscillation of $\nu_{C=S}$ and γ_{NH} groups. As for the IR spectra of thiolates **4**, the characteristic stretching vibrations of the $\nu_{C=S}$ group had a bathochromic shift at 14–40 cm^{-1} and these signals appeared at the range 1622–1613 cm^{-1}. This shift characterized the formation of an ionic bond between potassium and sulfur.

In the mass spectrum (electron impact, EI) of compound **3d**, the high-intensity molecular ion $M^{+\bullet}$ with ions $[M+1]^{+\bullet}$, $[M+2]^{+\bullet}$, and $[M-H]^{+\bullet}$ was presented. A further fragmentation by C(10b)–N(1) and N(3)–N(4) bonds was followed by formation of the thiophenamidine ion with *m/z* 124 and unstable thioquinazoline ion with *m/z* 161, which was characteristic of triazolo[1,5-*c*]quinazoline system cleavage. The ion with *m/z* 161 then consistently eliminated CNS and CHNS forming ions with *m/z* 103 (6.4 %) and 102 (9.9 %).

Mass spectra (EI) of amides **7c**, **7l**, and **7s** were characterized by low-intensity molecular ions $[M]^{+\bullet}$ with specific degradation of the amide fragment. Thus, for cycloalkylamide **7c** the most characteristic was α cleavage of the amide bond with formation of [Heteroaryl-SCH_2]$^+$ with *m/z* 297/298 (14.8/100.0 %); for benzylamide **7l**, α and β cleavage of bonds to [Heteroaryl-SCH_2]$^+$ with *m/z* 282/283 (32.8/6.2 %) and [Heteroaryl-S]$^+$ with *m/z* 269/270 (100.0/16.5 %); and for arylamide **7s**, formation of the ion [Heteroaryl-SCH_2CO]$^+$ with *m/z* 309 (100 %).

The IR spectra of acids **6** were different from the spectra of compounds **3**, namely, the presence of stretching vibrations of the associated ν_{NH} and ν_{OH} presented at 3419–3058 cm^{-1}, vibrations of the $\nu_{C=O}$ bond at 1766–1703 cm^{-1}, and of the $\gamma_{(OH\cdots O)}$ at 997–910 cm^{-1}. The IR spectra of amides **7** had two lines of stretching vibrations of the associated NH group at 3516–3008 cm^{-1}. The spectra of amides **7** were characterized by ν_{CO} (Amide I) at 1841–1633 cm^{-1} and mixed-valence deformation vibrations of NH and CN bonds (Amide II) at 1630–1510 cm^{-1}. Along with the key peaks of compounds **6** and **7** there were typical low-intensity peaks of aromatic ring C=C bonds at 1589–1468 cm^{-1}, low-intensity signals of ν_{S-R} at 2826–2500 cm^{-1}, nonplanar vibrations of $\gamma_{(=C-H)}$ at 850–666 cm^{-1}, and an intense absorption at 2960–2850 cm^{-1}, which belonged to the symmetric and asymmetric ν_{CH_3} and ν_{CH_2}.

The ^{1}H NMR spectra demonstrated the appropriate signals in the following ranges. The appearance of the low-field singlet of thioamide protons at $\delta = 14.04–13.82$ ppm and characteristic splitting on two one-proton doublets of triazolo[1,5-*c*]quinazoline: H-10 at $\delta = 8.33–8.23$ ppm and H-7 at $\delta = 7.69–7.65$ ppm, and two one-proton triplets: H-8 at $\delta = 7.82–7.65$ ppm and H-9 at $\delta = 7.55–7.47$ ppm, were in favor of compound **3** formation. In addition, compounds **3** were characterized by the functional substituent signals at position 2, which, depending on the structure, had classical magnetic shifts and the corresponding multiplicity.[15–18]

In the spectra of compounds **6** and **7**, the triazoloquinazoline fragment of molecules formed a characteristic subspectrum of two one-proton doublets: H-10 at $\delta = 8.48–8.35$ ppm and H-7 at $\delta = 7.97–7.83$ ppm, and two one-proton triplets: H-8 at $\delta = 7.85–7.60$ ppm and H-9 at $\delta = 7.67–7.60$ ppm. The data indicated that the chemical shifts of these protons differed from those of the parent compounds **3** and, as expected, they significantly affected the nature of the substituent at position 5. Protons of substituents at positions 2 and 5 in compounds **7** had classical multiplicity and chemical shifts determined by the existing substituents. Characteristic signals of acids **6** and amides **7** were two-proton singlets of the SC*H*$_2$ group at $\delta = 4.55–4.09$ ppm. The one-proton singlet of the –C(O)N*H* group in amides **7a**–**7e** resonated at $\delta = 8.44–7.73$ ppm and in amides **7r**–**7y** at $\delta = 11.90–9.73$ ppm. In amides **7j**–**7q** this proton signal appeared as a triplet or wide singlet at $\delta = 8.86–8.53$ ppm. Also in the spectra of **7j**–**7q**, a two-proton doublet of the C*H*$_2$Ph group was present at $\delta = 4.55–4.28$ ppm.

An interesting aspect in the ^{1}H NMR spectra of amides **7a**–**7i** was a shift of cycloalkyl or heterocyclyl protons to a strong magnetic field. Thus, spectra of **7a**–**7c**, which contained adamantine, had two six-proton singlets at $\delta = 1.67$ ppm (H-4′, 6′, 10′) and at $\delta = 1.98$ ppm (H-2′, 8′, 9′) and were associated with protons located near the bridging carbon atoms. A three-proton singlet at $\delta = 2.05$ ppm (H-3′, 5′, 7′) characterized the protons located at the nodal carbon atoms. A more complex picture was observed in the ^{1}H NMR spectrum of amide **7d**: axial and equatorial protons formed multiplets at $\delta = 1.59–0.90$, 1.74, 2.28–1.91, and 3.55–3.39 ppm. Protons of tetrahydrothienyl in amide **7e** were not equivalent and had a specific splitting, namely, they appeared as a doublet of doublets at $\delta = 4.56$ (H-3), 3.37 (H-2), 3.26 (H-5), 3.14 (H-5), 2.96, and 2.19 ppm (H-4).

The ^{13}C NMR spectra of compounds **7b** and **7d** were characterized by a significant unshielding of the carbon signal in position 5 ($\delta = 166.87–166.96$ ppm), which was a logical result of the electronegativity of sulfur.

Antimicrobial and antifungal activities

Starting and novel compounds were investigated for their in vitro antibacterial activity against *S. aureus, Pseudomonas aeruginosa*, and *E. coli* and antifungal properties against *C. albicans*. The research determined that quinazolinones **1** and phenylamines **2** showed a moderate antibacterial activity (see Table 1).

The exceptions were compound **1a** with a furan fragment and **2c** and **2d** with thien fragments, which exhibited a good inhibitive effect against *S. aureus* at a concentration of 25 μg mL^{-1}. The fungicidal and fungistatic effects of compounds **1** and **2** against *C. albicans* were also moderate (the minimal inhibitory concentration (MIC) and minimal fungicidal concentration (MFC) were 50–200 μg mL^{-1}).

The thiones **3** and their potassium salts **4** showed a high inhibitory and bacteri(fungi)cidal activity (MIC 50–100 μg mL^{-1}, minimal bactericidal concentration (MBC) and MFC 50–100 μg mL^{-1}) against strains of *E. coli*, *P. aeruginosa*, and *C. albicans* (Table 1). The most active compounds against *E. coli* strains were **3c**, **4h**, and **4i** (MIC 25 μg mL^{-1}), which contained thiophene, indole, and benzothiophene rings at the second position. However, compounds **3** and **4** were more effective against *S. aureus* (MIC 12.5–50 μg mL^{-1}). Hence, acetic acids **6** and amides **7a**–**7r** showed a moderate antibacterial activity (MIC 50–200 μg mL^{-1}).

Thus, modifications to thiones **3** to enhance their antibacterial activity had not led to the desired result. Introduction of the pharmacophore amine groups in substances **7** had a small positive impact on their antibacterial activity. The highest antimicrobial activity against *S. aureus* was for potassium thiolates **4**, as a result of their higher solubility in water than the corresponding thiones **3**, thus indicating the potential of their future research against methicillin-resistant *S. aureus* (MRSA) strains.

Moreover, the highest activity (MIC 12.5 μg mL^{-1}) was characteristic for derivatives that contain furan (**4a**, **4b**), thiophene (**4c**, **4d**), benzothiophene (**4h**), and indole (**4i**) cycles at the second position. So, substances **4a**–**4d**, **4h**, and **4i** were studied against MRSA at a concentration of 100 μg mL^{-1}. Unfortunately, only potassium 2-(2-furyl)-[1,2,4]triazolo[1,5-*c*]quinazoline-5-thiolate (**4a**) inhibited its growth to 7 mm.

Anticancer assay for preliminary in vitro testing

Some of the compounds (**1a**–**1d**, **1f**, **1h**, **1i**, **2a**–**2f**, **2h**, **2i**, **7e**–**7g**, **7k**, **7n**, **7p**, **7t**, **7u**, **7w**, **7x**) were selected according to the US National Cancer Institute (NCI) Developmental Therapeutic Program criteria for in vitro cell line screening to investigate their anticancer activity.[19] The compounds were firstly evaluated at one dose primary anticancer assay towards 60 cell lines (concentration 10^{-5} M). Average values of the dose-dependent antitumor activity main parameters against these cancer cell lines are shown in Table 2.

Table 1. Antimicrobial and antifungal activity data of the synthesized compounds [$\mu g\,mL^{-1}$].

Substance[a]	*E. coli*		*S. aureus*		*P. aeruginosa*		*C. albicans*		Substance[a]	*E. coli*		*S. aureus*		*P. aeruginosa*		*C. albicans*	
	MIC	MBC	MIC	MBC	MIC	MBC	MIC	MFC		MIC	MBC	MIC	MBC	MIC	MBC	MIC	MFC
1a	50	200	25	25	100	200	50	100	**3i**	50	50	25	50	100	200	100	100
1b	25	500	50	100	100	200	100	100	**4a**	50	100	12.5	25	50	200	50	100
1c	100	100	100	100	50	100	50	100	**4b**	100	100	12.5	25	100	200	50	100
1d	100	100	50	100	50	100	50	100	**4c**	100	100	12.5	25	100	200	100	100
1e	50	100	50	100	50	100	100	100	**4d**	50	100	12.5	25	100	200	50	100
1f	50	100	50	50	50	100	100	100	**4e**	50	100	50	100	100	200	100	100
1g	50	100	50	50	50	100	100	100	**4f**	50	100	100	100	100	200	100	100
2a	100	100	50	100	100	>200	100	100	**4g**	50	100	50	100	50	200	50	100
2b	50	100	50	100	100	200	100	100	**4h**	25	100	12.5	25	50	100	100	100
2c	50	100	25	50	100	200	50	100	**4i**	25	100	12.5	25	50	200	100	100
2d	50	100	25	100	100	200	50	50	**6a**	50	100	50	50	50	200	50	100
2e	100	100	50	100	100	>200	100	100	**6b**	50	100	50	50	50	200	50	100
2f	50	100	50	100	100	200	100	100	**6c**	50	100	50	50	50	200	50	100
2g	50	100	50	100	100	200	50	50	**6d**	50	100	50	50	50	200	50	100
2h	50	100	50	100	100	200	200	200	**7a**	100	100	100	200	50	200	100	100
2i	50	100	50	100	100	>200	100	>200	**7c**	50	100	100	200	100	200	50	100
3a	50	50	25	50	100	200	50	100	**7g**	100	100	100	200	50	200	50	100
3b	50	100	25	50	100	200	100	100	**7i**	100	200	50	200	100	100	200	200
3c	25	50	25	100	50	100	100	100	**7j**	50	100	100	200	50	200	100	100
3d	50	50	25	50	100	200	100	100	**7k**	100	100	100	200	50	200	100	100
3e	100	100	25	50	100	200	100	100	**7l**	100	100	200	200	50	100	100	100
3f	50	100	50	100	100	200	100	100	**7m**	100	100	100	200	50	100	100	100
3g	50	50	25	50	100	200	100	100	**7r**	100	100	100	500	50	200	100	100
3h	50	50	50	100	100	200	100	100	trimethoprim	50	50	31.2	62.5	62.5	125	62.5	125

[a] For **6e**–**6g**, **7b**, **7d**–**7f**, **7h**, **7n**–**7q**, **7s**-**7y** the minimal inhibitory concentration was $\geq 200\ \mu g\,mL^{-1}$. MIC = minimal inhibitory concentration, MBC = minimal bactericidal concentration, MFC = minimal fungicidal concentration.

The results showed that quinazoline-2-ones **1** had a narrow range of antitumor activity on the studied cancer cell lines. However, compounds **1a**–**1d** and **1h** effectively inhibited breast cancer (cell lines MCF7/BC, T-47D/BC, MDA-MB-231/ATCC, MDA-MB-468/BC) to 70%. Introduction, in position 2 of the triazoloquinazoline system, of the indole fragment for compound **1i** led not only to expansion of the spectrum (more than 30 cell lines), but also to a significant increase of activity. Transformation of compound **1** into the {2-[3-heteroaryl]-1*H*-[1,2,4-triazol-5-yl]phenyl}amines **2** resulted in narrowing of the activity spectrum and its reduction. Only for compound **2i**, with an indole cycle in position 3 of the triazole system, did growth inhibition increase to 30–80% against practically the entire spectrum of cancer cell lines (54 lines). Acetamides **7** were characterized by inhibition of the same breast cancer lines. Notably, compound **7g**, which also contains an indole ring in its structure, did not affect the growth of cancer cells significantly. Unfortunately substances **1f**, **2e**, and **7e** inhibited the growth of cancer cell lines by less than 30%.

Therefore, such preliminary antitumor activity data allowed us to obtain a number of validated pieces of evidence for its presence for {2-[3-(1*H*-indole-2-yl)-1*H*-1,2,4-triazol-5-yl]phenyl}-amine (**2i**) and to select this compound for the next phase of research by NCI protocols. According to the standard NCI phase II procedure of dose-dependency studies, compound **2i** was investigated at five concentrations in tenfold dilution (100–0.01 μм) at 59 lines of nine cancer cell types (Figure 1, Table 3).

Note the high sensitivity of all cancer cell lines to compound **2i** (MG MID $\log GI_{50} = -5.49$). Substance **2i** shows high activity against cell lines K-562 of leukemia, NCI-H522 of non-small-cell lung cancer, KM12 of epithelial colon cancer, SF-295 of central nervous system (CNS) cancer, ACHN, CAKI-1, and UO-31 of renal cancer, MDA-MB-231/ATCC of breast cancer, and LOX IMVI, M14, and MDA-MB-435 of melanoma. In addition, compound **2i** had a high cytostatic effect against cell lines NCI-H522 of non-small-cell lung cancer, HCC-2998 and KM12 of epithelial colon cancer, SF-295 of CNS cancer, LOX IMVI, M14, MDA-MB-435, and UACC-62 of melanoma, UO-31 of renal cancer, and MDA-MB-468 of breast cancer. As for the cytotoxic effect, compound **2i** showed it in higher concentrations against cell lines NCI-H522 of non-small-cell lung cancer, HCC-2998 and KM12 of colon cancer, M14, MDA-MB-435, and UACC-62 of melanoma, and UO-31 of renal cancer.

The conducted structure–activity relationship analysis of the anticancer activity revealed a number of critical "pharmacophore" fragments and determined the optimal directions of further molecule modification. Hence, it was established that anticancer properties were influenced by the nature of the substituent in position 2 of the [1,2,4]triazolo[1,5-*c*]quinazoline cycle, which increased in the series: pyrrole-2-yl < thiophene-3-yl < benzothiophene-2-yl < thiophene-2-yl < furan-2-yl < substituted pyrrole-5-yl < benzofuran-2-yl < furan-3-yl < indole-2-yl.

Docking studies to *S. aureus* dihydrofolate reductase

To elucidate the possible antimicrobial activity mechanism, it was decided to conduct molecular docking to dihydrofolate reductase (DHFR) because it is crucial for the biosynthesis of pu-

Table 2. Percentage of in vitro tumor cell line growth at 10 μM.

Substance	Growth range	The most sensitive cell line growth[a]
1a	29.07–125.05	68.61 (A498/r), 68.67 (UO-31/r), 29.07 (MCF7/b), 67.36 (T-47D/b)
1b	26.89–122.27	26.89 (MCF7/b), 50.41 (T-47D/b), 33.42 (MDA-MB-468/b)
1c	59.34–108.82	59.34 (COLO 205/c), 66.37 (HT29/c), 69.49 (SNB-75/n), 69.42 (UO-31/r), 61.03 (T-47D/b)
1d	64.13–137.29	64.13 (UO-31/r)
1h	49.85–127.25	66.83 (IGROV1/o), 49.85 (UO-31/r), 62.09 (MCF7/b), 69.25 (T-47D/b)
1i	44.81–109.05	61.84 (CCRF-CEM/l), 52.29 (K-562/l), 67.52 (A549/ATCC/s), 64.83 (NCI-H322M/s), 52.74 (NCI-H522/s), 59.99 (KM12/c), 68.35 (SF-295/n), 53.13 (LOX IMVI/m), 48.95 (UACC-62/m), 64.90 (ACHN/r), 66.02 (CAKI-1/r), 44.81 (UO-31/r), 66.67 (MDA-MB-231/ATCC/b), 55.28 (T-47D/b)
2a	54.39–144.29	54.39 (MCF7/b)
2b	22.91–150.10	66.65 (SNB-75/n), 65.65 (UO-31/r), 22.91 (MCF7/b), 48.07 (T-47D/b)
2c	53.99–145.11	65.37 (SNB-75/n), 64.50 (IGROV1/o), 53.99 (UO-31/r)
2d	56.69–178.62	59.19 (SNB-75/n), 66.91 (IGROV1/o), 56.69 (UO-31/r)
2f	51.87–131.55	60.02 (K-562/l), 51.87 (MOLT-4/l), 61.01 (UO-31/r)
2h	36.21–106.68	57.76 (CCRF-CEM/l), 51.24 (MOLT-4/l), 66.61 (SR/l), 66.52 (EKVX/s), 64.60 (NCI-H322M/s), 61.88 (NCI-H522/s), 66.52 (SNB-75/n), 65.87 (UACC-62/m), 44.60 (IGROV1/o), 56.90 (CAKI-1/r), 36.21 (UO-31/r), 62.09 (PC-3/PC), 66.36 (MCF7/b)
2i	9.71–92.87	42.62 (CCRF-CEM/l), 37.91 (HL-60(TB)/l), 15.42 (K-562/l), 47.73 (MOLT-4/l), 29.23 (SR/l), 33.11 (A549/ATCC/s), 60.45 (EKVX/s), 51.28 (NCI-H322M/s), 47.74 (NCI-H460/s), 37.36 (HCC-2998/c), 53.68 (HCT-116/c), 40.41 (HCT-15/c), 19.23 (KM12/c), 47.51 (SW-620/c), 66.23 (SF-268/n), 52.31 (SF-295/n), 62.77 (SF-539/n), 86.05 (SNB-19/n), 60.60 (SNB-75/n), 67.65 (U251/n), 31.97 (LOX IMVI/m), 46.25 (MALME-3M/m), 13.67 (MDA-MB-435/m), 57.64 (SK-MEL-2/m), 47.88 (SK-MEL-5/m), 9.71 (UACC-62/m), 33.50 (IGROV1/o), 53.08 (OVCAR-3/o), 51.21 (OVCAR-4/o), 52.42 (OVCAR-5/o), 57.03 (OVCAR-8/o), 42.04 (NCI/ADR-RES/o), 50.10 (A498/r), 44.66 (ACHN/r), 15.73 (CAKI-1/r), 60.40 (SN12C/r), 69.23 (TK-10/r), 32.61 (UO-31/r), 43.88 (PC-3/PC), 59.82 (MCF7/b), 51.07 (T-47D/b)
7f	67.35–112.68	67.35 (HOP-92/s)
7g	55.92–111.69	55.92 (OVCAR-4/o), 69.50 (MDA-MB-231/ATCC/b)
7l	26.25–121.20	68.43 (NCI-H460/s), 44.32 (HCT-116/c), 54.42 (SNB-75/n), 40.70 (OVCAR-4/o), 31.35 (MCF7/b), 53.12 (MDA-MB-231/ATCC/b), 67.34 (T-47D/b), 26.25 (MDA-MB-468/b)
7n	48.28–119.71	67.00 (SNB-75/n), 48.28 (MCF7/b), 60.49 (MDA-MB-231/ATCC/b), 68.51 (MDA-MB-468/b)
7p	36.27–116.33	65.39 (IGROV1/o), 62.81 (UO-31/r), 36.27 (MCF7/b), 59.44 (T-47D/b), 71.21 (MDA-MB-468/b)
7u	39.81–117.29	67.71 (SF-539/n), 39.81 (MCF7/b), 67.23 (T-47D/b), 52.55 (MDA-MB-468/b)
7t	1.47–116.80	43.44 (HCT-15/c), 67.36 (KM12/c), 66.39 (OVCAR-4/o), 14.37 (MCF7/b), 68.58 (MDA-MB-231/ATCC/b), 36.37 (T-47D/b)
7w	51.63–119.44	51.63 (SNB-75/n) 67.93 (MDA-MB-231/ATCC/b), 65.59 (HS 578T/b)
7x	60.20–114.74	60.20 (MCF7/b)

[a] Only more than 30% inhibition effect is shown. l=leukemia, s=non-small-cell lung cancer, c=colon cancer, n=central nervous system cancer, m=melanoma, o=ovarian cancer, r=renal cancer, p=prostate cancer, b=breast cancer.

rines, thymidylate, and some amino acids, and furthermore synthesized [1,2,4]triazolo[1,5-*c*]quinazolines are condensed structural analogues of 2,4-diaminoquinazolines, which are reported to have a high selectivity to *S. aureus* DHFR.[20]

The flexible molecular docking study was performed by using the geometry-optimized structure of the investigated compounds into the active site of *S. aureus* DHFR (4LAE.pdb) with the software package OpenEye.[21–23] Trimethoprim and 7-(2-ethoxynaphthalen-1-yl)-6-methylquinazoline-2,4-diamine were used as the references.[20] The obtained scoring functions (Shapegauss, PLP, Chemgauss2, Chemgauss3, Chemscore, OE-Chemscore, Screenscore, CGO, CGT, Zapbind, Consensus Score) indicated the best possibility of matching into the ligand–protein complex (Table S1 in the Supporting Information).

On analyzing the results, practically half of the substances had better Consensus Scores than the two references (Table S1). Unexpectedly, the best affinity was shown by substances with the largest heterocyclic fragments: *N*-(2-chlorobenzyl)-2-(2-(1-benzothienyl-2))- (**7p**), *N*-(2-chlorophenyl)-2-(2-(1-benzothienyl-2))- (**7x**), *N*-(4-chlorobenzyl)-2-(2-(thienyl-3))- (**7n**), *N*-(2-bromobenzyl)-2-(2-(1-benzofuran-2-yl))- (**7o**), and *N*-(4-bromophenyl)-2-{[2-(1-benzofuran-2-yl)-[1,2,4]triazolo[1,5-*c*]quinazoline-5-yl]thio}acetamide (**7w**), owing to the appropriate hydrophobic intercalation into the active site of *S. aureus* DHFR. Visual inspection of the substance **7p** (B) with practically ten times better Consensus Score than that of the reference quinazoline derivative (A) is demonstrated in Figure 2.

The poorest results were found for 2-heteroaryl-[1,2,4]triazolo[1,5-*c*]quinazoline-5(6*H*)-ones **1** and 2-(3-heteroaryl-1*H*-1,2,4-triazol-5-yl)anilines **2**. Potassium salts **4** also had poor results.

By comparing the molecular docking results with in vitro screening, we could suppose that the presumed antibacterial mechanism is not of DHFR inhibition. To predict it more concisely, various docking studies with subsequent enzyme analysis should be done. Considering the fact of high antibacterial activity against *S. aureus*, thiolates **4a**–**4i** will be investigated and the results reported in another paper.

Docking studies to epidermal growth factor receptor kinase

It has been reported that several quinazoline derivatives—Erlotinib, Gefitinib, Afatinib, and Icotinib—are epidermal growth factor receptor (EGFR) tyrosine kinase inhibitors, and they are currently available as treatment for patients with advanced non-small-cell lung cancer with EGFR mutations.[24] So, to predict the possible anticancer activity mechanism, the investigated substances were also molecularly docked to epidermal growth factor receptor kinase (EGFRK) (1m17.pdb).[21–26] Gefiti-

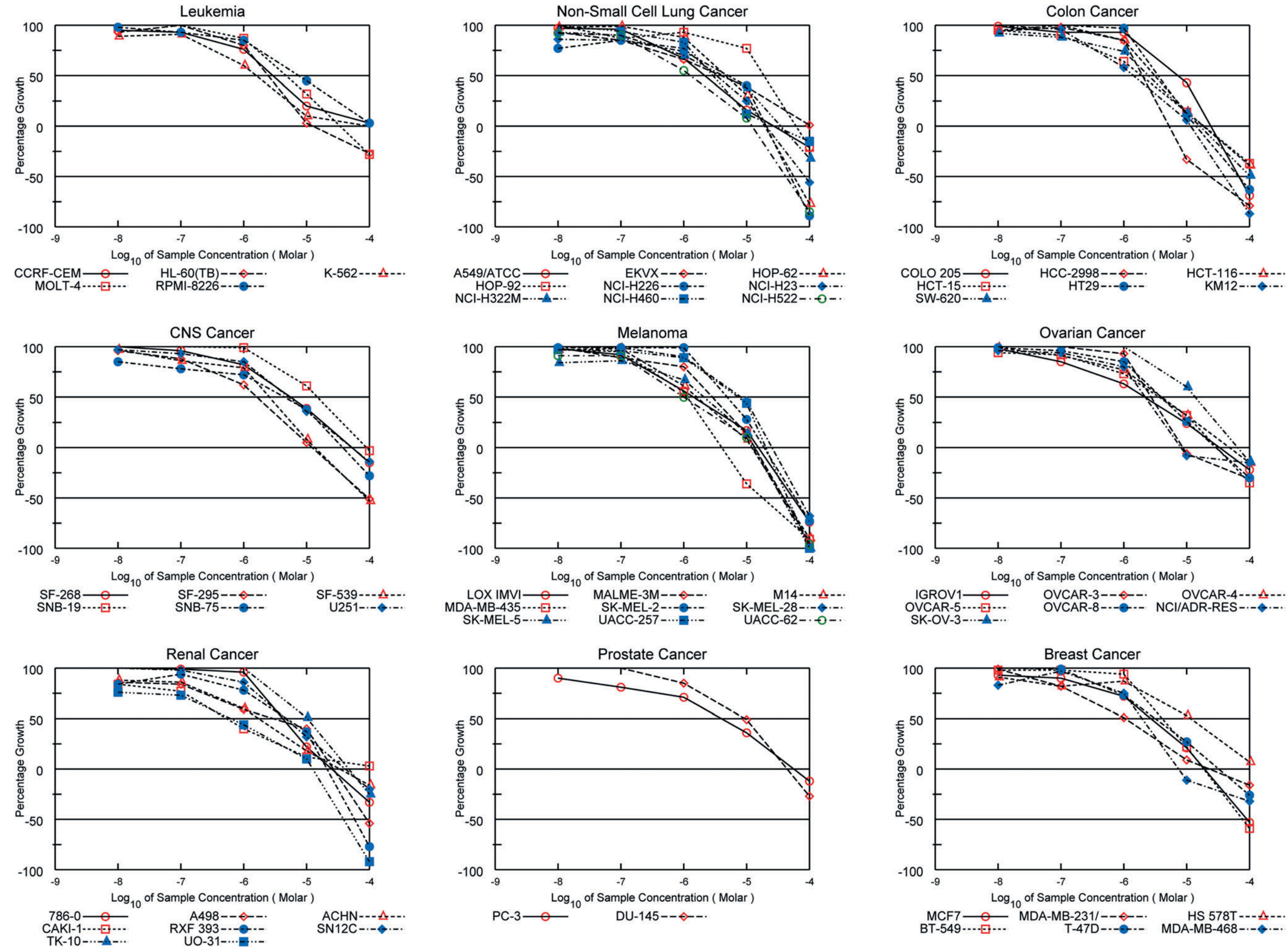

Figure 1. Graphs of the anticancer activity of **2i** at the 59 lines of nine cancer cell types in tenfold dilution (100–0.01 μM).

Table 3. Compound **2i** anticancer data against individual tumor lines ($\log GI_{50} > 5.70$).

Cell line/cancer type	Log GI_{50}	Log TGI	Log LC_{50}
K-562/leukemia	−5.80	> −4.00	> −4.00
NCI-H522/non-small-cell lung	−5.89	−4.92	−4.38
HCC-2998/colon	−5.70	−5.28	−4.64
HCT-15/colon	−5.71	−4.72	> −4.00
KM12/colon	−5.84	−4.93	−4.40
SF-295/CNS	−5.79	−4.90	−4.02
LOX IMVI/melanoma	−5.85	−4.81	−4.27
M14/melanoma	−5.79	−4.92	−4.41
MDA-MB-435/melanoma	−5.94	−5.40	−4.75
UACC-62/melanoma	−6.00	−4.91	−4.44
ACHN/renal	−5.77	−4.48	> −4.00
CAKI-1/renal	−6.26	−4.00	> −4.00
UO-31/renal	−6.20	−4.90	−4.41
MDA-MB-231/ATCC/breast	−5.98	−4.64	> −4.00
MDA-MB-468/breast	−5.71	−5.13	> −4.00
MG MID—average data	−5.49	−4.60	−4.11

GI_{50} = growth inhibition of 50%, TGI = total growth inhibition, LC_{50} = concentration lethal to 50%.

nib (*N*-(3-chloro-4-fluoro-phenyl)-7-methoxy-6-(3-morpholin-4-yl-propoxy)quinazolin-4-amine) was used as a reference.[24]

It was found that *N*-(4-fluorophenyl)- (**7v**) and *N*-(4-bromophenyl)-2-{[2-(1-benzofuran-2-yl)-[1,2,4]triazolo[1,5-*c*]quinazoline-5-yl]thio}acetamide (**7w**) had Consensus Scores three times better (98 and 90) than that of Gefitinib (311; Table S2). As seen in the visual representation, owing to the rotation by the sulfur bond, substance **7w** effectively located its substituent in the EGFRK pocket (Figure 3).

No hydrogen bonds were formed between the investigated substances and enzyme. Still, 19 substances had better affinity to the EGFRK active site than Gefitinib. Except for the already mentioned ones, among them were 13 amides, bearing thienyl-3(2), benzothienyl-2, furan-2-yl, adamantyl, piperidin-1-yl (and so forth) fragments, two acetic acids with 2-(1-benzofuran-2-yl) (**6e**) and 2-(1*H*-indol-2-yl) (**6g**) residues, 2-(3-(benzo[*b*]thiophen-2-yl)-1*H*-1,2,4-triazol-5-yl)aniline **2h**, and 2-(benzo[*b*]thiophen-2-yl)-[1,2,4]triazolo[1,5-*c*]quinazoline-5(6*H*)-thione **3h**. The compounds with lower results had other functional derivatives, which were less substituted. The main impact on the presence of affinity was made by the larger heteroaryl substituent, plane structure of the [1,2,4]triazolo[1,5-*c*]quinazoline skeleton, and rotation possibility of the radicals. Amides **7** once more appeared to have more affinity.

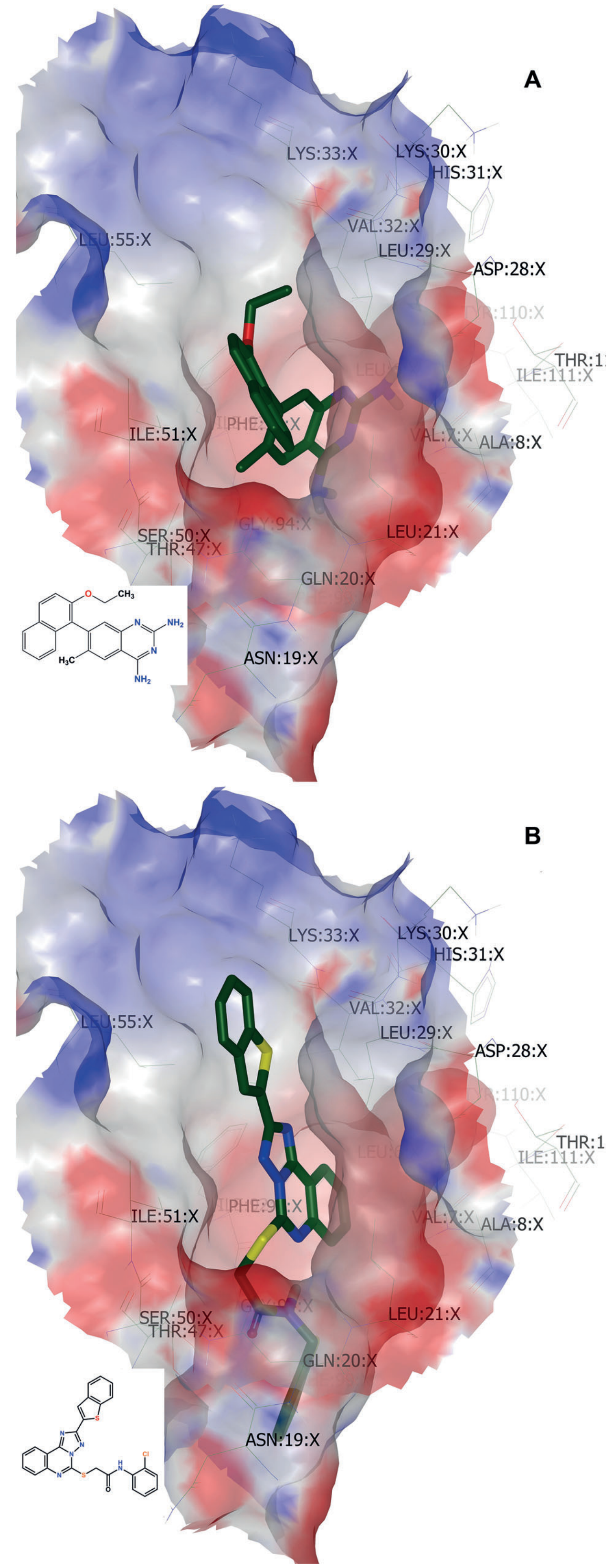

Figure 2. Visual representation of a receptor–ligand interaction: active site of *S. aureus* dihydrofolate reductase (4LAE.pdb) and 7-(2-ethoxynaphthalen-1-yl)-6-methylquinazoline-2,4-diamine (A), reference compound, and *N*-(2-chlorobenzyl)-2-{[2-(1-benzothienyl-2)-[1,2,4]triazolo[1,5-*c*]quinazoline-5-yl]-thio}acetamide (**7 p**, B), which has the highest Consensus Score.

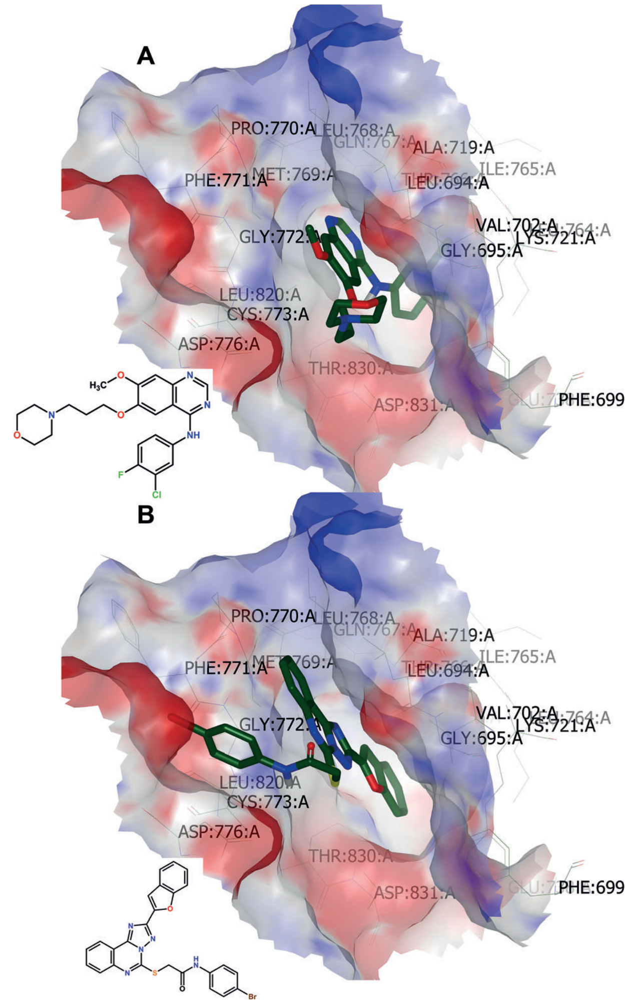

Figure 3. Visual representation of a receptor–ligand interaction: active site of epidermal growth factor receptor tyrosine kinase (1m17.pdb) and Gefitinib (A) and *N*-(4-bromophenyl)-2-{[2-(1-benzofuran-2-yl)[1,2,4]triazolo[1,5-*c*]quinazoline-5-yl]thio}acetamide (**7 w**, B), which has the highest Consensus Score.

On analyzing the anticancer in vitro investigation results, it can be suggested that amides **7** could have EGFRK inhibition properties, but substances of series **1** and **2** ought to have another mechanism of activity. Still, it should be proved by direct enzyme study.

Conclusion

To synthesize, novel antimicrobial and anticancer agents, several methods for preparing 2-heteroaryl-[1,2,4]triazolo[1,5-*c*]quinazoline-5(6*H*)-ones(thiones) and their S-substituted derivatives were developed. The structures of the synthesized compounds were evaluated by ^{1}H and ^{13}C NMR spectroscopy, LC–MS, EIMS, and elemental analysis. In vitro antibacterial activity tests against *Staphylococcus aureus*, *Pseudomonas aeruginosa*, and *Escherichia coli*, and antifungal activity against *Candida albicans* demonstrated that some potassium 2-heteroaryl-[1,2,4]triazole[1,5-*c*]quinazoline-5-thiolates (**4 a**–**4 d**, **4 h**, **4 i**) possessed high antibacterial activity against *S. aureus* with minimal inhibitory concentration of 12.5 μg mL^{-1} and minimal bactericidal concentration of 25 μg mL^{-1}, as a result of their hydrophilic properties, which increased the bioavailability.

Practically all of the compounds had no effect on MRSA. Molecular docking scores to *S. aureus* dihydrofolate reductase did not correlate with in vitro activity results, which suggested another activity mechanism. US National Cancer Institute in vitro screening revealed {2-[3-(1*H*-indole-2-yl)-1*H*-1,2,4-triazol-5-yl]-phenyl}amine (**2i**) had anticancer potential as in the I and II phases of the investigations it showed a GI_{50} of 3.12–7.03 μM and total growth inhibition of 15.56–67.38 μM. Considering the epidermal growth factor receptor kinase docking studies, series **7** could have such inhibition properties, but **1** and **2** must have another mechanism of activity. Hence, the best structure modification for biologically active substances appeared to be introduction of the 1*H*-indole-2-yl fragment either in the {2-[3-heteroaryl]-1*H*-1,2,4-triazol-5-yl]phenyl}amine or in 2-heteroaryl-[1,2,4]triazole[1,5-*c*]quinazoline-5(6*H*)-thiolate.

Hence, the search for anticancer agents among {2-[3-(1*H*-indole-2-yl)-1*H*-1,2,4-triazol-5-yl]phenyl}amine derivatives will be continued through the search for the optimal combination of the benzene substituents in the indole and quinazoline rings: alkyl, halogeno, trifluoromethyl, alkoxy, and so forth. The same aspect was used to enhance and expand the activity of 4-anilinoquinazolines, the known kinase inhibitors.[27–32]

Antimicrobial and antifungal tests

Investigation of the antimicrobial activity was performed by serial dilutions in Muller–Hinton broth. The substance (1 mg) was dissolved in dimethyl sulfoxide (DMSO, 1 mL). Then dilutions at a concentration of 200 μg mL^{-1} (for *S. aureus* ATCC 25923, *E. coli* ATCC 25922, *P. aeruginosa* ATCC 27853) and methicillin-resistant *Staphylococcus* strain in 100 μg mL^{-1} or in Sabouraud broth (for *C. albicans* ATCC 885–653) were prepared by addition of 1 mL of the last mentioned solution to 4 mL of the appropriate broth. Then a set of serial dilutions was prepared in 1 mL solution. Microbial inoculum (0.1 mL) was added to each test tube. Inoculum with an optical density of 0.5 by the MakFarland standard (1.5×10^8 cfu mL^{-1}; cfu = colony-forming unit) was prepared in saline from clearly isolated colonies of microorganisms that grew in dense nutrient medium after 16–18–24 h of incubation. The microbial colonies were diluted 100 times in the nutrient broth (10^6 cfu mL^{-1}). Inoculum (0.1 mL, 10^5 cfu mL^{-1}) was added to the test tube within 15 min after the investigated substance dilution. The test tubes with *S. aureus*, *E. coli*, and *P. aeruginosa* were incubated at (37 ± 1) °C for 16–24 h, and those with *C. albicans* at (28 ± 1) °C for 44–48 h. Experiments were accompanied by a "negative" control comprising 1 mL of nutrient broth without antibiotic and 0.1 mL of inoculum (10^5 cfu mL^{-1}).

The minimum inhibition concentration (MIC) was determined by the absence of visible in vitro growth in the test tube with a minimum concentration of the substance. The minimum bactericidal concentration (MBC) was determined by the absence of visible in vitro growth at the Muller–Hinton agar after the addition of 0.1 mL of mixture from the transparent test tubes. The minimum fungicidal concentration (MFC) was determined by the absence of visible in vitro growth at the Sabouraud agar after the addition of 0.1 mL of mixture from the transparent test tubes.

Experimental Section

Chemistry

General methods: Melting points were determined in open capillary tubes and were uncorrected. Elemental analyses (C, H, N, S) were performed using the ELEMENTAR vario EL Cube analyzer (USA). Analyses were indicated by the symbols of the elements or functions within ±0.3% of the theoretical values. IR spectra (4000–600 cm^{-1}) were recorded on a Bruker ALPHA FTIR spectrometer (Bruker Bioscience, Germany) using a module for measuring attenuated total reflection (ATR). ^{1}H NMR spectra (400 MHz) and ^{13}C NMR spectra (100 MHz) were recorded on a Varian-Mercury 400 (Varian Inc., Palo Alto, CA, USA) spectrometer with TMS as internal standard in [D$_6$]DMSO solution. LC–MS was recorded using a system consisting of a high-performance liquid chromatograph (Agilent 1100 Series; Agilent, Palo Alto, CA, USA) equipped with a diode-matrix and mass-selective detector (Agilent LC/MSD SL; atmospheric-pressure chemical ionization). Electron-impact (EI) mass spectra were recorded on a Varian 1200L instrument at 70 eV (Varian, USA). The purity of all obtained compounds was checked by ^{1}H NMR spectroscopy and LC–MS.

Substances **1a**–**1g** and **2a**–**2i** were synthesized according to the reported procedures.[5,15–18] Other starting materials and solvents were obtained from commercially available sources and used without additional purification.

Synthesis, yields, characterization data, and examples of **3a**, **3b**, **6c**, and **7c** spectra are given in the Supporting Information, Appendix 1.

Anticancer screening

Primary anticancer assay was performed at a human tumor cell lines panel derived from nine neoplastic diseases, in accordance with the protocol of the Drug Evaluation Branch, National Cancer Institute, Bethesda.[19] Tested compounds were added to the culture at a single concentration (10^{-5} M) and the cultures were incubated for 48 h. End point determinations were made with a protein-binding dye, sulforhodamine B (SRB). Results for each tested compound were reported as the percent of growth of the treated cells when compared to the untreated control cells. The percentage growth was evaluated spectrophotometrically versus controls not treated with test agents. The cytotoxic and/or growth inhibitory effects of the most active selected compounds were tested in vitro against the full panel of about 60 human tumor cell lines at tenfold dilutions of five concentrations ranging from 10^{-4} to 10^{-8} M. A 48 h continuous drug exposure protocol was followed and an SRB protein assay was used to estimate cell viability or growth. Using the seven absorbance measurements [time zero (T_z), control growth in the absence of drug (C), and test growth in the presence of drug at the five concentration levels (T_i)], the percentage growth was calculated at each of the drug concentrations levels. Percentage growth inhibition was calculated as [Eqs. (1) and (2)]:

$$[(T_i - T_z)/(C - T_z)] \times 100 \text{ for concentrations for which } T_i \geq T_z \quad (1)$$

$$[(T_i - T_z)]/T_z] \times 100 \text{ for concentrations for which } T_i < T_z \quad (2)$$

Three dose–response parameters were calculated for each compound. Growth inhibition of 50% (GI_{50}) was calculated from $[(T_i-T_z)/(C-T_z)]\times100=50$, which is the drug concentration resulting in a 50% lower net protein increase in the treated cells (measured by SRB staining) relative to the net protein increase seen in the control cells. The drug concentration resulting in total growth inhibition (TGI) was calculated from $T_i=T_z$. The LC_{50} value (concentration of drug resulting in a 50% reduction in the measured protein at the end of the drug treatment as compared to that at the beginning) indicating a net loss of cells following treatment was calculated from $[(T_i-T_z)/T_z]\times100=-50$. Values were calculated for each of these three parameters if the level of activity was reached; however, if the effect was not reached or was exceeded, the value for that parameter was expressed as greater or less than the maximum or minimum concentration tested. The $\log GI_{50}$, $\log TGI$, and $\log LC_{50}$ were then determined, defined as the mean of the log values of the individual GI_{50}, TGI, and LC_{50} values. The lowest values were obtained with the most sensitive cell lines.

Docking, scoring, and visual inspection of synthesized substances into the enzyme binding sites

Flexible molecular docking was performed using the software package OpenEye, including related utilities: Fred Receptor 2.2.5, Vida 4.1.1, Flipper, Babel 3, Omega 2.4.3, and Fred 2.2.5.[22,23] The crystal structures of the *S. aureus* DHFR (4LAE.pdb) and EFGRK (1m17.pdb) were obtained from the protein data bank.[21]

The methodology of research consisted of the following steps. 1) Generation of *R*, *S*, and *cis–trans* isomers of ligands (the studied compounds and relevant drugs, program Flipper), which allowed the production of the studied compounds' isomer range. 2) Molecular modeling (Hyper Chem 7.5) by generation of the 3D structures of the obtained isomeric forms using the method of molecular mechanics (MM+) and the semiempirical quantum mechanical method with Polak–Ribiere algorithm (PM3). 3) Generation of ligand conformations (Omega 2.4.3). The number of obtained conformations was not significant owing to the further selection of the most optimal conformers by program Fred 2.2.5. 4) Carrying out molecular docking (Fred 2.2.5). Scoring functions (Shapegauss, PLP, Chemgauss 2, Chemgauss 3, Chemscore, OEChemscore, Screenscore, CGO, CGT, Zapbind, Consensus Score) were obtained as a result of studies, values of which assess specific characteristics of the ligand–protein complex, thereby indicating the possibility of their matching.

Acknowledgements

We gratefully acknowledge Enamine Ltd. (Kiev, Ukraine) for the financial support of this study, and we thank the team of the Drug Synthesis and Chemistry Branch, National Cancer Institute, Bethesda, MD, USA, for in vitro evaluation of anticancer activity.

Keywords: antibacterial agents · antifungal agents · antitumor agents · biological activity · heterocycles

[1] *Chemistry of Heterocyclic Compounds, Vol. 24* (Ed.: W. L. F. Armarego), Wiley, New York, **2008**, p. 518.
[2] J. P. Michael, *Nat. Prod. Rep.* **2005**, *22*, 627–646.
[3] K. Špirková, Š. Stankovský, M. Dandárová, *Collect. Czech. Chem. Commun.* **1994**, *59*, 222–226.
[4] S. A. Shiba, A. A. El-Khamry, M. E. Shaban, K. S. Atia, *Pharmazie* **1997**, *52*, 189–194.
[5] M. A. El-Hashash, S. A. Rizk, F. A. El-Bassiouny, K. M. Darwish, *Global Journal of Health Science* **2012**, *4*, 174–183.
[6] Y. Zheng, M. Bian, X.-Q. Deng, S.-B. Wang, Z.-S. Quan, *Arch. Pharm.* **2013**, *346*, 119–126.
[7] N. U. Lin, E. P. Winer, D. Wheatley, L. A. Carey, S. Houston, D. Mendelson, *Breast Cancer Res. Treat.* **2012**, *133*, 1057–1065.
[8] H. A. Burris III, *Oncologist* **2004**, *9*, 10–15.
[9] N. Mauras, L. G. de Pijem, H. Y. Hsiang, P. Desrosiers, R. Rapaport, *J. Clin. Endocrinol. Metab.* **2008**, *93*, 823–831.
[10] A. K. Gupta, F. C. Simpson, *Skin Therapy Lett.* **2014**, *19*, 1–4.
[11] J. Heeres, R. Hendrickx, J. Van Cutsem, *J. Med. Chem.* **1983**, *26*, 611–613.
[12] T. F. Patterson, H. W. Boucher, R. Herbrecht, D. W. Denning, O. Lortholary, P. Ribaud, *Clin. Infect. Dis.* **2005**, *41*, 1448–1452.
[13] L. G. Bahrin, M. O. Apostu, L. M. Birsa, M. Stefan, *Bioorg. Med. Chem. Lett.* **2014**, *24*, 2315–2318.
[14] S. Kima, R. Kubec, R. A. Musah, *J. Ethnopharmacol.* **2006**, *104*, 188–192.
[15] L. N. Antipenko, A. V. Karpenko, S. I. Kovalenko, A. M. Katzev, E. Z. Komarovska-Porokhnyavets, *Arch. Pharm. Chem. Life Sci.* **2009**, *342*, 651–662.
[16] L. N. Antipenko, A. V. Karpenko, S. I. Kovalenko, A. M. Katzev, E. Z. Komarovska-Porokhnyavets, A. A. Chekotilo, *Chem. Pharm. Bull.* **2009**, *57*, 580–585.
[17] A. V. Karpenko, S. I. Kovalenko, S. V. Shishkina, O. V. Shishkin, *Monatsh. Chem.* **2006**, *137*, 1543–1549.
[18] S. I. Kovalenko, L. M. Antypenko, A. K. Bilyi, S. V. Kholodnyak, O. V. Karpenko, O. M. Antypenko, N. S. Mykhaylova, T. I. Los', O. S. Kolomoets', *Sci. Pharm.* **2013**, *81*, 359–391.
[19] http://www.dtp.nci.nih.gov.
[20] T. Lam, M. T. Hilgers, M. L. Cunningham, B. P. Kwan, K. J. Nelson, V. Brown-Driver, V. Ong, M. Trzoss, G. Hough, K. J. Shaw, J. Finn, *J. Med. Chem.* **2014**, *57*, 651–668.
[21] Protein Data Bank, pdb. [http://www.pdb.org].
[22] *PART V: Docking Strategies and Algorithms, Virtual Screening in Drug Discovery*, (Eds.: J. Alvarez, B. Shoichet), CRC Press, Taylor & Francis, Boca Raton, **2005**, pp. 301–348.
[23] Fred Receptor 2.2.5, Vida 4.1.1, Flipper, Babel 3, Omega 2.4.3 and Fred 2.2.5: OpenEye Sci. Soft. Inc. Santa Fe, NM, USA, **2011**. [http://www.eyesopen.com].
[24] J.-K. Lee, S. Hahn, D.-W. Kim, K. J. Suh, B. Keam, T. M. Kim, S.-H. Lee, D. Seog Heo, *JAMA* **2014**, *311*, 1430–1437.
[25] L.-J. Liu, K.-H. Leung, D. S.-H. Chan, Y.-T. Wang, D.-L. Ma, C.-H. Leung, *Cell Death Differ.* **2014**, *5*, e1293.
[26] D. L. Ma, D. S. Chan, G. Wei, H. J. Zhong, H. Yang, L. T. Leung, E. A. Gullen, P. Chiu, Y. C. Cheng, C. H. Leung, *Chem. Commun.* **2014**, *50*, 13885–13888.
[27] V. Bavetsias, J. H. Marriott, C. Melin, *J. Med. Chem.* **2000**, *43*, 1910–1926.
[28] L. Shewchuk, A. Hassell, B. Wisely, *J. Med. Chem.* **2000**, *43*, 133–138.
[29] C. Cao, J. M. Albert, L. Geng, *Cancer Res.* **2006**, *66*, 11409–11415.
[30] A. E. Wakeling, S. P. Guy, J. R. Woodburn, S. E. Ashton, B. J. Curry, A. J. Barker, K. H. Gibson, *Cancer Res.* **2002**, *62*, 5749–5754.
[31] G. E. Konecny, M. D. Pegram, N. Venkatesan, *Cancer Res.* **2006**, *66*, 1630–1639.
[32] M. W. Karaman, S. Herrgard, D. K. Treiber, *Nat. Biotechnol.* **2008**, *26*, 127–132.

Received: February 4, 2015
Revised: February 12, 2015
Published online on ■■ ■■, 0000

Killer instinct: In the search for effective biologically active heterocycles, it has been found that potassium 2-heteroaryl-[1,2,4]triazolo[1,5-*c*]quinazoline-5-thiolates have high antibacterial activity against *Staphylococcus aureus*. In addition, {2-[3-(1*H*-indole-2-yl)-1*H*-1,2,4-triazol-5-yl]phenyl}amine has high anticancer activity in terms of 50 % and total growth inhibition (see figure).

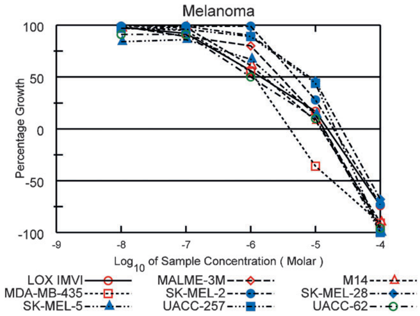

*A. K. Bilyi, L. M. Antypenko, V. V. Ivchuk, O. M. Kamyshnyi, N. M. Polishchuk, S. I. Kovalenko**

■■ – ■■

2-Heteroaryl-[1,2,4]triazolo[1,5-*c*]quinazoline-5(6 H)-thiones and Their S-Substituted Derivatives: Synthesis, Spectroscopic Data, and Biological Activity